Deep-ultraviolet Raman spectroscopy study of the effect of aging on human cortical bone

J. W. Ager III
R. K. Nalla
K. L. Breeden
Lawrence Berkeley National Laboratory
Materials Sciences Division
Berkeley, California 94720

R. O. Ritchie
Lawrence Berkeley National Laboratory
Materials Sciences Division
Berkeley, California 94720
and
University of California
Department of Materials Science and Engineering
Berkeley, California 94720

Abstract. The age-related deterioration in bone quality and consequent increase in fracture incidence is an obvious health concern that is becoming increasingly significant as the population ages. Raman spectroscopy with deep-ultraviolet excitation (244 nm) is used to measure vibrational spectra from human cortical bone obtained from donors over a wide age range (34–99 years). The UV Raman technique avoids the fluorescence background usually found with visible and near-infrared excitation and, due to resonance Raman effects, is particularly sensitive to the organic component of bone. Spectral changes in the amide I band at 1640 cm^{-1} are found to correlate with both donor age and with previously reported fracture toughness data obtained from the same specimens. These results are discussed in the context of possible changes in collagen cross-linking chemistry as a function of age, and are deemed important to further our understanding of the changes in the organic component of the bone matrix with aging.
[DOI: 10.1117/1.1924668]

Keywords: Cortical bone; aging; Raman spectroscopy; fracture toughness.

Paper 04140RR received Jul. 22, 2004; revised manuscript received Nov. 10, 2004; accepted for publication Dec. 13, 2004; published online Jun. 1, 2005.

1 Introduction

It is well known that the susceptibility to bone fracture increases with age;[1] indeed, much work has focused on the mechanisms of bone deterioration responsible for this elevated fracture risk.[2] Bone mass or bone mineral density (BMD) has traditionally been used as a clinical predictor of such fracture risk. However, there is mounting evidence that BMD alone may not be the sole factor responsible for the aging-induced fracture risk.[1,3,4] For example, work by Hui et al.[1] reported a roughly tenfold increase in fracture risk with aging in a sample group in which the BMD remained practically unchanged. Consequently, in an effort to develop a more complete understanding, a number of studies have investigated the influence of several factors (e.g., anatomical location, mineral density, porosity, collagen quality, mineral physicochemistry, etc.) on the evolution of the strength and toughness properties of bone with age in both human and animal subjects.[5–18]

Understanding the mechanical properties of bone will require studies that probe over multiple dimensions owing to the complex, hierarchical structure of bone.[19–21] At the macrostructural level, bone is distinguished into cortical (compact) and cancellous (trabecular) bone; most long bones are composed of a cortical shell with a cancellous interior. At microstructural length scales, cortical bone is organized into 200–300 μm diameter secondary osteons,[21] which are composed of large vascular channels (50–90 μm diameter) surrounded by circumferential lamellar rings (3–7 μm thick), with so-called ''cement lines'' at the outer boundary.[20] These secondary osteons are the end result of the remodeling process that repairs damage *in vivo* and are believed to be involved in the toughening of bone.[22] At the nanostructural level, the lamellae are composed of organic type-I mineralized collagen fibers (up to 15 μm in length, 50–70 nm in diameter, and formed by regular arrangement of subnanostructural collagen molecules) bound and impregnated with inorganic carbonated apatite nanocrystals (tens of nanometers in length and width, 2–3 nm in thickness).[19]

Over the past two decades, a number of vibrational spectroscopy techniques, including infrared (IR) absorption and reflectance (e.g., Refs. 23–32), Raman scattering (e.g., Refs. 16 and 33–37), and inelastic neutron scattering (e.g., Refs. 38 and 39), have been used to study both the organic and inorganic components of bone. Carden and Morris[40] report on a recent and comprehensive review of Raman and IR studies in this area. Spectroscopic studies have targeted issues that include mineralization (e.g., Refs. 25 and 39), disease (e.g., Refs. 26 and 28), aging (e.g., Refs. 16, 23, 24, 29, 31, and 33), and mechanical deformation (e.g., Refs. 35). Although IR-based techniques are relatively more well established, Raman spectroscopy, with its finer (~1 μm in a Raman microprobe) spatial resolution, is increasingly being used.[40] Sample fluorescence, which can obscure the Raman scattering signal, can be a problem in performing *in situ* studies of bone and other biological samples with visible laser excitation. Near-IR excitation (see Ref. 40 and references cited therein) and sophisticated background subtraction methodologies[35] have been used

Address all correspondence to R. O. Ritchie. Tel: (510) 486-5798; Fax: (510) 486-4881; E-mail: RORitchie@lbl.gov

1083-3668/2005/$22.00 © 2005 SPIE

successfully to partially avoid this problem in bone samples.

Surprisingly though, there are relatively few studies that have used vibrational spectroscopy to specifically study age-related changes in the bone matrix. Fourier transform infrared spectroscopy (FTIR) and Raman studies focused on the mineral component have revealed some small changes in the mineral content, crystallinity and chemical nature.[16,23,24,33] Paschalis et al.[31] reported age-related changes in the amide I band in bovine bone (it is unclear whether trabecular/cortical bone was used), which were associated with an increase in the nonreducible (trivalent) pyridinoline (Pyr) cross links and a decrease in the reducible (divalent) dehydrodihydroxylysinonorleucine (deH-DHLNL) cross links. Very et al.[29] investigated small age-related changes in the amide bands in the FTIR spectrum of human trabecular bone and found that, with increasing age, the amide peaks shifted to slightly lower energies and the relative intensities of the high energy components of the amide I band decreased with age.

However, most spectroscopic studies have not correlated the subnanostructural information gained from the vibrational spectra directly to the mechanical properties, and in particular the fracture resistance, of the bone specimen under study. Here, we show that the use of ultraviolet excitation eliminates fluorescence interference and allows nondestructive *in situ* measurements of Raman spectra from human cortical bone. Due to resonance effects, peaks associated with the bone organic component (particularly the amide I band) are selectively enhanced. Significant changes in the shape of the amide bands are found, which are correlated both with age of the bone donor and with the fracture properties of the specific bone specimen. The null hypothesis offered here is that the amide I band can be resonance-enhanced through the use of deep-UV excitation and that its shape is affected by aging.

2 Materials and Methods

2.1 *Materials*

Freshly frozen cadaveric cortical bone, obtained according to protocols approved by the Lawrence Berkeley National Laboratory and the University of California at Berkeley, was taken from the mid-diaphyseal sections of the humeri of nine human donors whose cause of death was unrelated to their skeletal state. The donors ranged in age from 34–99 years; the individual donor information (and number of specimens from each donor) is summarized in Table 1. The bone was sectioned into rectangular blocks 15–20 mm×15–20 mm ×1.2–3 mm thick. All surfaces of the blocks were polished to a 1200 grit finish, followed by polishing steps using a 1 μm alumina suspension, and finally a 0.05 μm alumina suspension.[22] Full details of specimen selection and preparation have been described in detail elsewhere in the context of the fracture toughness testing of bone.[18–22] These blocks were used to make compact-tension fracture toughness specimens, oriented such that crack growth occurs in the proximal-distal orientation. The toughness tests were performed prior to the spectroscopy work.

Table 1 Donor information for human humeral cortical bone.

Age (years)	Sex	Arm	No. of specimens
Young (34–41 years)			
34	Female	Left	2
37*	Male	Left	2
37*	Male	Right	1
41	Female	Left	2
Middle-Aged (61–69 years)			
61	Male	Left	2
69	Female	Left	2
69	Female	Right	2
Aged (85–99 years)			
85	Female	Right	1
85	Female	Right	2
99	Male	Right	2

* Specimens taken from same donor.

2.2 *UV Raman Spectroscopy*

A continuous wave intracavity doubled, argon ion laser operating at 244 nm was used as the excitation source for the UV Raman spectroscopy. The laser power at the sample was kept below 5 mW, and a custom-made rotating (~45 rpm) stage was used to prevent laser damage to the organic component of the bone matrix. [UV lasers do have the potential to damage organic matter. When higher laser power (15 mW and above) were used, particularly in the absence of sample spinning, changes in the spectrum with time that could be attributed to collagen degradation. To avoid such artifacts, laser power was kept under 5 mW and the samples spun continuously. Micro-FTIR (data not reported here) performed before and after deep-UV exposure, revealed no changes in the spectra.] The laser was focused to a ~500 μm spot on the surface of the bone samples with an f/4 100 mm fused silica lens. Backscattered light was collected with the same lens, collimated, and directed to the entrance slit of a triple spectrometer optimized for performance in the deep-UV regime. The instrument dispersion used was 2.1 cm^{-1}/pixel. The instrument resolution was varied between 15 and 30 cm^{-1} by adjusting the slit width of the dispersion stage of the triple spectrometer. These measurement established that the linewidths of the major features in the spectrum (e.g., of the well-resolved CH_2 wag) were 40 cm^{-1} and higher. Reported data were obtained at 30 cm^{-1} instrument resolution to maximize sensitivity without artificially broadening the lines. Spectra were collected with a liquid nitrogen cooled, backthinned CCD camera. Ten frames of 10 s exposure each were collected; comparison of the first and last frames from each set confirmed that there was no sample degradation under laser illumination. Spectral calibration was performed with the known Raman line positions of cyclohexane.

2.3 *Spectrum Processing and Data Analysis*

Each data collection set of ten frames was considered to be an independent measurement and were averaged with cosmic ray

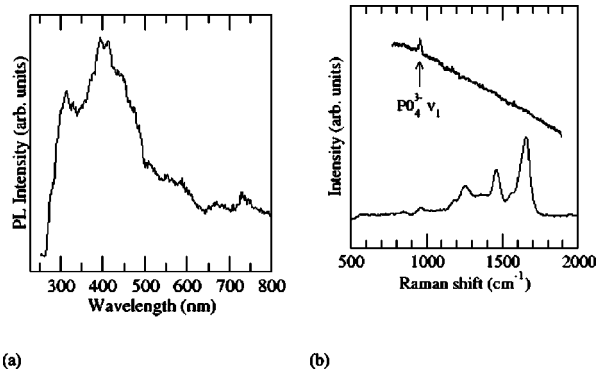

Fig. 1 (a) Photoluminescence spectrum of human bone excited with 244 nm laser light and detected with single spectrometer, photomultiplier, and lock-in amplifier. Strong fluorescence exists throughout the visible and into the near-IR regime. However, the fluorescence signal is low between the laser wavelength and 260 nm, enabling Raman shifts of up to 2500 cm^{-1} to be observed with low background. (b) Comparision of Raman spectra obtained with 244 nm (bottom) and 632.8 (top) nm light. Strong fluorescence background obscures all but the strongest peak (phosphate ν_1) in the visible (632.8 nm) Raman spectrum.

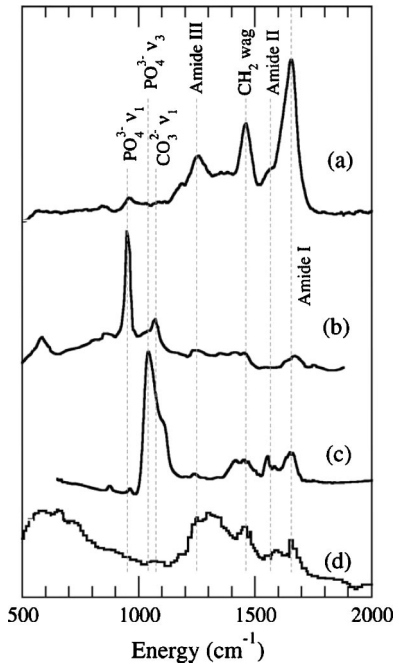

Fig. 2 Comparison of vibrational spectra of bone obtained with different spectroscopic techniques: (a) ultraviolet Raman spectrum of human bone, this work; (b) near infrared Raman spectrum of bovine bone;[41] (c) IR reflectance of human bone, this work; (d) inelastic neutron scattering of ox femur.[30] Strong inorganic (phosphate and carbonate) and organic (amide I, II, and III and CH_2 wag) are noted. Measurement conditions were reported as follows: (a) UV Raman, 244 nm, 500 mm spot size, <5 mW laser power, 100 second collection time, subtraction of small, linear background; (b) near-IR Raman, 1064 nm excitation, 650 mW laser power, 4 cm^{-1} resolution, white light corrected; (c) FTIR obtained in reflectance with 4 cm^{-1} resolution, using same sample as in (a); (d) 2.5 powdered sample, 12 h collection time.

events removed. A small linear background was defined by the signal at 500 and 2000 cm^{-1} (where little Raman scattering from the sample is expected) and subtracted. Spectra were normalized to the height of the CH_2 wag peak at ~1460 cm^{-1} and smoothed with a nine-point running average. It was possible to describe the observed spectra between 800 and 1800 cm^{-1} with 10 overlapping Gaussian lines [a number of line shapes (Gaussian, Voight, Lorenzian) were tested for spectral fitting; the smallest residuals were obtained with Gaussian lines], including broad peaks centered at 1070 and 1380 cm^{-1}. However, the most pronounced spectra changes between specimens were found in the amide I band. For specific analysis of this region, nonlinear least-squares fitting to four features centered at ~1460 cm^{-1} (CH_2 wag), 1580 cm^{-1} (amide II), 1610 cm^{-1} (amide I), and 1655 cm^{-1} (amide I) was employed. The mean position and normalized height/area of these peaks are reported as averages from all specimens taken from a single donor (see Table 1). Linear regression analysis was performed for peak position and peak area against donor age ($P<0.05$ is considered significant, $0.05<P<0.10$ weakly significant, and $P>0.10$ not significant).

3 Results

3.1 *UV Raman Spectroscopy*

Figure 1(a) shows the fluorescence spectrum from 250 to 800 nm obtained from human cortical bone under 244 nm (deep-UV) excitation. Evidently, the fluorescence is strong throughout the visible region of the spectrum and well into the near-IR regime. However, with 244 nm excitation, Stokes Raman shifts between 500 and 2000 cm^{-1} are observed between 247 and 256 nm. The bulk of the fluorescence occurs to the red of this wavelength range. Hence, as shown in Fig. 1(b), it is possible to obtain Raman spectra with a very low background that does not substantially interfere with the collection of the vibrational spectrum of interest. Data obtained separately from a similar human bone sample with 632.8 nm (visible) excitation are shown in Fig. 1(b) for comparison; due to strong fluorescence interference, only the phosphate ν_1 peak can be observed. Although we do not know if UV excites fluorescence more effectively than visible light and indeed, the short absorption length of the deep-UV light might cause the effective fluorescence signal to be smaller due to the smaller volume of material excited, deep-UV excitation was found to enable low-background Raman spectroscopy *in spite* of strong fluorescence.

Figure 2 compares vibrational spectra from bone samples (human and animal) obtained with UV Raman, near-IR Raman, IR reflectance, and inelastic neutron scattering. The near-IR spectrum obtained using 1064 nm excitation, from Smith and Rehman,[41] is dominated by the phosphate ν_1 and other inorganic features [Fig. 2(b)]. In fact, the strength and narrow linewidth of this feature has enabled it to measure changes in mineral content of bone in the context of mechanical deformation.[35] The FTIR spectrum [Fig. 2(c)] is similar to that of the near-IR Raman spectrum, except that the carbonate features are dominant. Although a number of groups have previously reported spectra obtained with visible and near IR lasers (530–785 nm) in which fluorescence does not appear to be a problem, for the material studied here 632.8 nm excitation produced spectra in which only one peak (phosphate ν_1) was definitively observable, as shown in Fig. 1(b). Whether

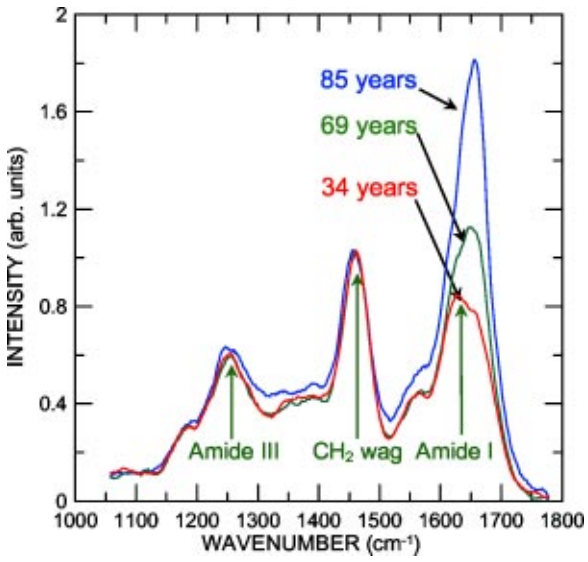

Fig. 3 UV Raman spectra of human humerus bone from donors of three different ages. The relative height of the amide I feature compared to the CH_2 wag is larger in the sample from the older donor, and there is a positional shift of this band to higher energies with aging.

near-IR excitation might reduce the background further in our samples remains to be investigated. Clearly, the organic features (amides I, II, and III and the CH_2 wag) are resonance enhanced and are typically more prominent than the inorganic features in the UV Raman spectrum. This spectrum resembles that obtained from inelastic neutron scattering [Fig. 2(d)], a technique which is more sensitive to vibrations with significant hydrogen motion.[39] Deep-UV excitation thus leads to very distinct, well-defined, resonance-enhanced Raman peaks from the organic matrix, with almost complete absence of fluorescence, and without the need for demineralization, making it an excellent candidate for nondestructive spectroscopic evaluation of bone and other mineralized tissues. Thus, the combination of visible Raman for careful measurement of the inorganic component and of the organic/inorganic ratio and UV Raman for detailed matrix analysis might be a powerful tool to probe such tissues.

3.2 *Spectral Analysis*

Figure 3(a) shows data in the organic portion of the spectrum ($\sim$1100–1800 cm^{-1}) for three representative specimens. To the authors' knowledge, these are the first Raman spectra from mineralized biological tissues such as bone that utilized a deep-ultraviolet laser excitation source. The spectra were all normalized to the height of the CH_2 wag peak, the position (and height) of which was observed to be practically invariant with age and across donors/specimens. In particular, three organic bands are strongly resonance enhanced and definitively identified here—amide III (primarily from the in-phase combination of NH in-plane bend and CN stretch, $\sim$1245–1260 cm^{-1}), CH_2 wag ($\sim$1454–1461 cm^{-1}) and amide I (primarily from the C═O stretch, $\sim$1626–1656 cm^{-1}). The amide II band (primarily from the out-of-phase combination of NH in-plane bend and CN stretch) that is sometimes seen in IR spectra at $\sim$1540–1580 cm^{-1} (Ref. 40) was rather weak in the present data (Fig. 3), presumably as it was not as strongly resonance enhanced.

Large changes in peak shape were observed for the amide I band, particularly in the spectra from the very elderly donors (85–99 years). When the band is considered as a whole, it appears that its center frequency shifts by as much as $\sim$20 cm^{-1} (Fig. 3). The amide III and CH_2 wag bands did not show significant variations in band position (less than $\sim$2 cm^{-1}). The amide I band also showed variations in intensity with age (Fig. 3). The changes in band shape were made more quantitative by fitting the amide I region to overlapping Gaussian peaks as described in Sec. 2.3. (We do not know *a priori* if changes in the underlying structure of the band produce the observed shifts in its apparent center frequency or whether it is the opposite, that is, that the shifts in the band center cause the changes in the underlying structure.) The results of this procedure are shown in Fig. 4 in which four individual peaks—one each corresponding to the CH_2 wag and the amide II bands, and two for the amide I band—are used to fit the spectra between 1400 and 1800 cm^{-1}.

Peak fitting results from all spectra were evaluated using linear regression analysis against age and fracture toughness data. The peak position of all four fit peaks was only weakly correlated with age. Figure 5 shows peak areas for the two peaks underlying the amide I band ($\sim$1610 and 1655 cm^{-1}) against age. The areas of both peaks showed good correlation with age ($r=-0.6138$ and 0.6570 for peaks at 1610 and 1655 cm^{-1}, respectively), as did the ratio of the areas ($r=-0.6026$). The area of these peaks show some significant variation with age ($P=0.0787$ and 0.0545 for peaks at 1610 and 1655 cm^{-1}, respectively), as do the ratio of the areas, 1610/1655 cm^{-1} ($P=0.0858$). The changes in the ratios of the peak areas are consistent with shift in the center of the amide I band; it appears that an increase in the intensity of the higher energy (1655 cm^{-1}) feature in samples from older donors is responsible for the evident shift of the center of the asymmetric amide I band.

4 Discussion

The amide bands, particularly amides I and III, are believed to be good indicators of protein conformation because of the role of the amide moiety in cross linking and bonding.[42] Examination of the present data shows that both the height and location of the resonance-enhanced amide I band vary with age (Fig. 3), supporting the proposed null hypothesis. The band center position moves to a higher energy with increasing age due to the larger contribution from the high energy component, as was evident when the underlying peaks were analyzed [Fig. 5(c)].

We had previously demonstrated the effect of aging on the fracture toughness ''resistance curve'' (R curve) behavior of human cortical bone using the same specimens used here and reported decreases in both the crack-initiation and crack-growth toughnesses that were correlated with donor age.[18] [Although the use of a single-value measure of the fracture toughness is appropriate for certain materials, in many ductile and brittle materials, including cortical bone,[22] the fracture resistance actually increases with crack extension, requiring a resistance curve (R curve) fracture-mechanics approach.[43,44]

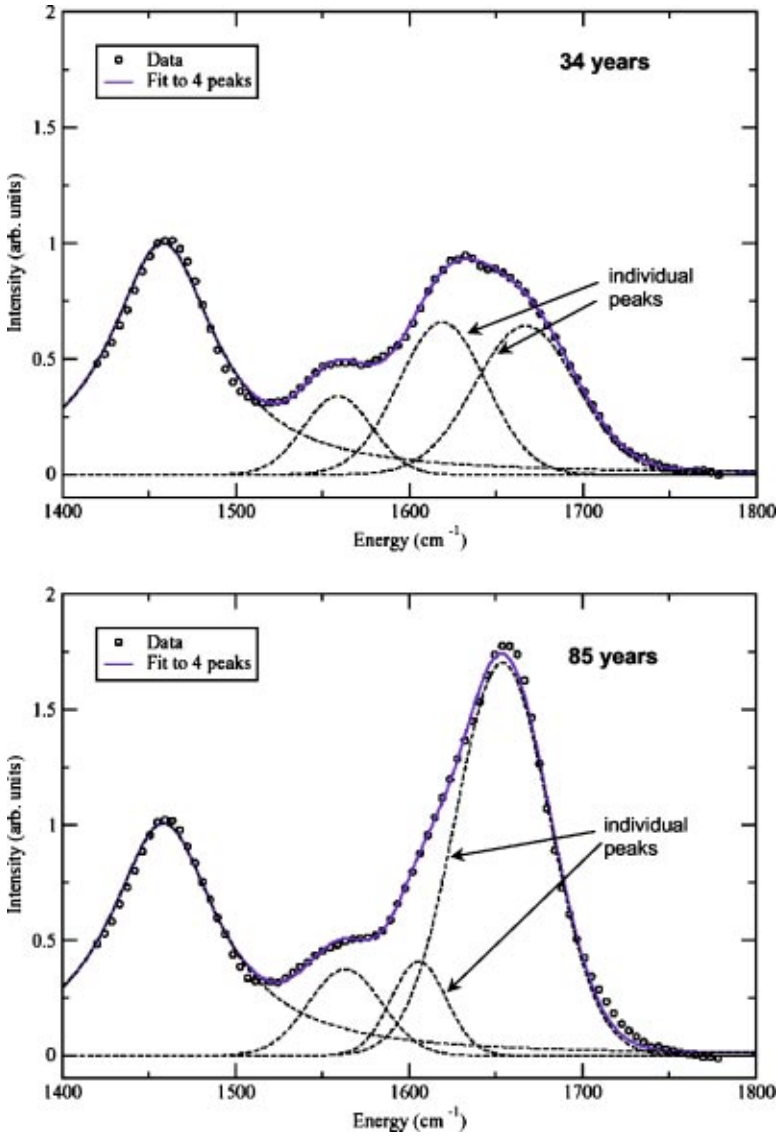

Fig. 4 Details of the peak fitting to the CH_2 wag and amide I region of the UV Raman spectrum for human cortical bone from a young (top) and old (bottom) donor. A good description of the spectrum is found by nonlinear least squares fitting to four peaks centered at ~1450 cm^{-1} (CH_2 wag), 1510 cm^{-1} (amide II), and 1610 and 1655 cm^{-1} (amide I with underlying structure). The donor age is indicated in each case.

In particular, *R* curves are necessary to describe the fracture resistance of materials toughened by crack-tip shielding,[45–47] i.e., mechanisms such as crack bridging or constrained microcracking, which develop in the crack wake as the crack extends. In such instances, crack extension commences at a *crack-initiation toughness*, and with further crack extension requires a higher driving force until typically a ''plateau'' or steady-state toughness is reached. The corresponding slope of the *R* curve can be considered as a measure of the *crack-growth toughness*.] Both measures of the toughness are needed for a complete understanding of the fracture resistance of materials such as cortical bone that show evidence of extrinsic toughening.[18,22] [Crack propagation can be considered as a mutual competition between two classes of mechanisms: *intrinsic* mechanisms, which are microstructural damage mechanisms that operate ahead of the crack tip and promote crack growth, and *extrinsic* mechanisms, which act to ''shield'' the crack from the applied driving force and operate principally in the wake of the crack tip to inhibit crack growth.[45–47]] Linear regression analyses of the area ratio of the 1610 and 1655 cm^{-1} peaks (the two peaks underlying the amide I band as observed in deep-UV Raman spectroscopy) against crack-initiation and crack-growth toughness are shown in Fig. 6. A more significant correlation is seen in the case of the crack-initiation toughness ($r=0.69$ and $P=0.04$) compared to the crack-growth toughness ($r=0.44$ and $P=0.23$). These results suggest that the ''quality'' of the collagen has a stronger influence on crack-initiation toughness as opposed to crack-propagation toughness.

We have previously demonstrated that the crack-growth toughness in cortical bone is primary the result of the extrinsic toughening mechanism of crack bridging.[22] The primary source of such bridging in human bone appears to be the

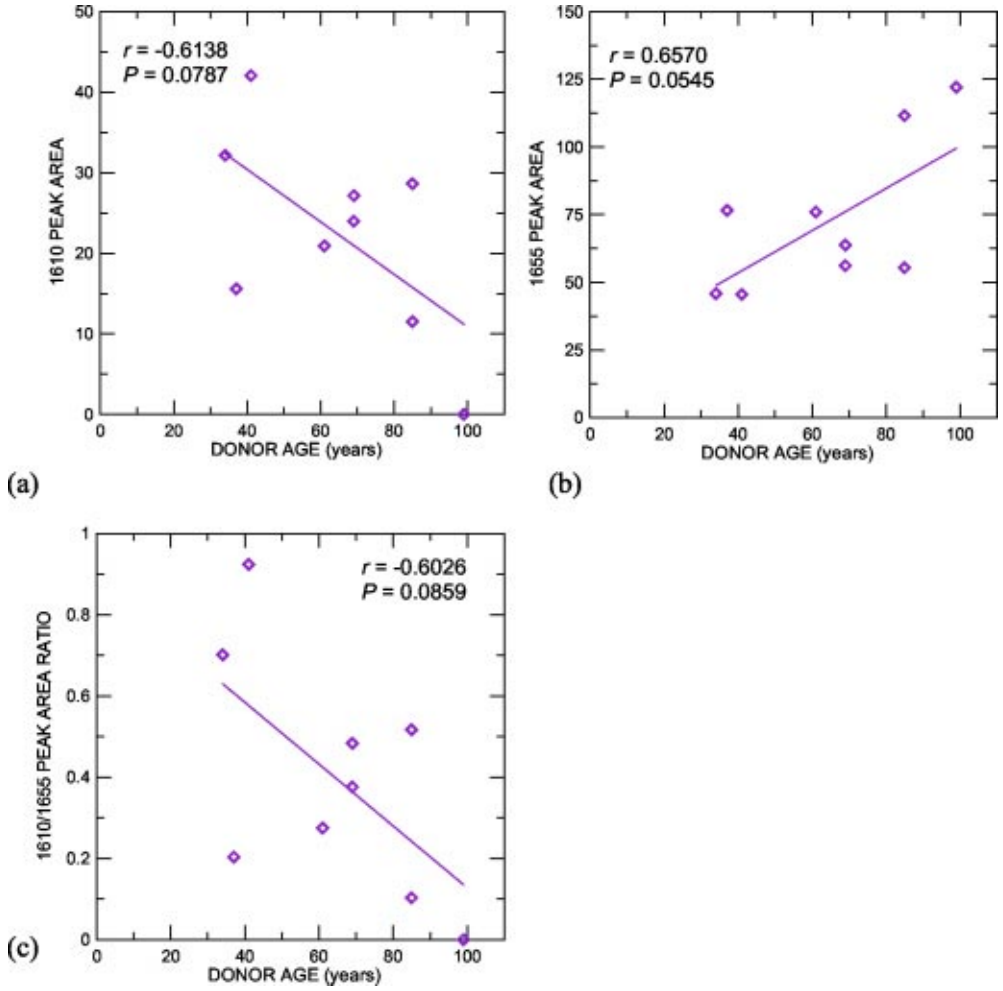

Fig. 5 Variation in the area of the two peaks (~1610 and 1655 cm^{-1}) underlying the amide I band with donor age. The correlation coefficient, *r*, and the *P* value for significance are included in each plot and a linear regression of the data is also shown. The "area" was defined as the product of the height and the full width at half-maximum (FWHM) of the peak.

formation of so-called uncracked ligaments in the crack wake,[18,22] which are essentially ''bridges'' of material spanning the crack behind the crack tip. These are created either by the nonuniform advance of the crack front and/or by the imperfect linking of microcracks ahead of the crack tip with the main crack. Our previous observations showed that cracks growing in bone were deflected around the osteons, and propagated preferentially along the presumably weaker cement lines. Such behavior would imply that the tissue microstructure would be expected to play a more important role in older bone and is consistent with our previous observations that the more extensive remodeling in older bone[48] leads to lower amounts of extrinsic toughening by crack bridging, and hence, lower crack-growth toughness.[18] Consequently, it is not surprising that more significant correlations were found in the case of the crack-initiation toughness, rather than the crack-growth toughness, as we can presume that the former is more strongly affected by the collagen quality. Thus, these results show that when considering the effect of aging in mineralized tissues, it is important to account for not just the changes at nanostructural dimensions, but also at the microstructural level.

At the molecular (subnanostructural) level, it has been suggested that the deleterious effects of aging can be attributed to changes in the cross-linking chemistry in bone.[49,50] Changes in the nature of the cross linking are known to affect the biomechanical properties of bone.[51] Although most studies looking at age-related changes in the cross linking have utilized high-performance liquid chromatography (e.g., Refs. 12, and 52–54), Paschalis et al.[31,32] have deconvoluted FTIR spectroscopic data into overlapping component peaks to probe the secondary structures in bone collagen. These authors reported that two peaks at ~1660 and 1690 cm^{-1} underlying the amide I band are particularly indicative of the cross linking, with the area ratio between them (1660/1690) corresponding to the nonreducible/reducible cross-link ratio. This ratio was observed to increase with age in demineralized bovine bone. Our data did not reveal an underlying peak at ~1690 cm^{-1}; this component of the amide I band is not resonance enhanced. However, we did observe an aging-induced increase in the contribution of a peak at ~1655 cm^{-1}, consistent with an increase in the nonreducible (Pyr) cross-link content in bone (Fig. 4). It has also been suggested that, with time, the reducible DHLNL matures into the nonreducible Pyr cross

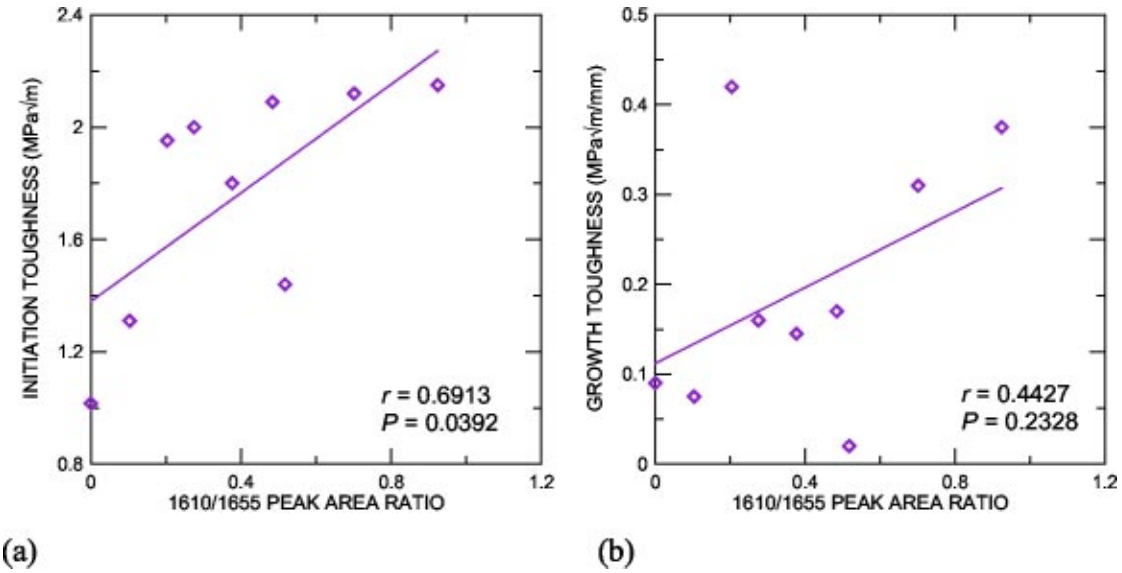

Fig. 6 Variation in the crack initiation and growth toughness with peak area ratio for the 1610 and 1655 cm^{-1} peaks underlying the amide I band. The correlation coefficient, *r*, and the *P* value for significance are included in each plot and a linear regression of the data is also shown.

link, leading to an increase in the content of the latter.[55] These results imply that the protein conformation in the organic matrix (which is ~90–95% collagen) does indeed change with age. More detailed studies with appropriate purified peptide standards are currently being undertaken to quantify such changes.

In summary, we have used deep-UV Raman spectroscopy to show that aging affects the organic component of the human cortical bone, in particular the amide I band. Moreover, we have demonstrated that deep-UV excitation leads to very distinct, well-defined Raman bands from the organic matrix, with almost complete absence of fluorescence, and without the need for demineralization; the technique is therefore an excellent candidate for nondestructive spectroscopic evaluation of mineralized tissues. Spectral changes are also directly correlated, for the first time, to the mechanical properties, more specifically, to the crack-initiation and crack-growth fracture toughness. However, it must be noted that a limitation of this study is the relatively small sample size, specifically 18 specimens taken from 9 separate donors. More detailed investigations which look at the specific effects of variables such as gender, anatomical location, microstructural variations, and bone mineral density, are required to obtain a more complete understanding and are currently being undertaken. Although we took precautions to minimize microstructural variations by extracting the specimens from roughly the same positions from all the humeri used, and the relatively large laser spot size (together with the use of a rotating stage) helps sample a substantial portion of each specimen thereby eliminating bias from local microstructural variations, we expect that some of the variables listed above contributed to the observed scatter. Clearly, further investigations are necessary to assess how aging-related changes affect bone at the subnanostructural levels, particularly to define the cross-linking chemistry and the consequent effect on ''bone quality.'' Such an approach is important from the perspective of gaining a full understanding of the effects of aging on the fracture resistance of mineralized tissues.

Acknowledgments

This work was supported by the National Institutes of Health under Grant No. 5R01 DE015633 [for one of the authors (R.K.N.)], and by the Director, Office of Science, Office of Basic Energy Science, Division of Materials Sciences and Engineering, Department of Energy under Contract No. DE-AC03-76SF00098 [for two of the authors (J.W.A.) and (R.O.R.)]. One of the authors (K.L.B.) was supported by the High School Student Participation Program through the LBNL Center for Science and Engineering Education. All of the authors acknowledge Professor A. P. Tomsia for his continued support, Professors J. H. Kinney, J. W. Ager, Jr., and J. J. Kruzic for many useful discussions, Dr. Y. Borodko for use of the UV Raman system, and Drs. C. Puttlitz and Z. Xu for supply of the cortical bone.

References

1. S. L. Hui, C. W. Slemenda, and C. C. Johnston, ''Age and bone mass as predictors of fracture in a prospective study,'' *J. Clin. Invest.* **81**, 1804–1809 (1988).
2. G. M. Kiebzak, ''Age-related bone changes,'' *Exp. Gerontol.* **26**, 171–187 (1991).
3. T. J. Aspray, A. Prentice, T. J. Cole, Y. Sawo, J. Reeve, and R. M. Francis, ''Low bone mineral content is common but osteoporotic fractures are rare in elderly rural gambian women,'' *J. Bone Miner. Res.* **11**, 1019–1025 (1996).
4. R. Heaney, ''Is the paradigm shifting?'' *Bone (N.Y.)* **33**, 457–465 (2003).
5. C. U. Brown, Y. N. Yeni, and T. L. Norman, ''Fracture toughness is dependent on bone location—a study of the femoral neck, femoral shaft, and the tibial shaft,'' *J. Biomed. Mater. Res.* **49**, 380–389 (2000).
6. P. Zioupos and J. D. Currey, ''Changes in the stiffness, strength, and toughness of human cortical bone with age,'' *Bone (N.Y.)* **22**, 57–66 (1998).
7. A. Burstein, D. Reilly, and M. Martens, ''Aging of bone tissue me-

chanical properties,'' *J. Bone Jt. Surg.* **58A**, 82–86 (1976).
8. J. B. Phelps, G. B. Hubbard, X. Wang, and C. M. Agrawal, ''Microstructural heterogeneity and the fracture toughness of bone,'' *J. Biomed. Mater. Res.* **51**, 735–741 (2000).
9. J. D. Currey, ''Changes in impact energy absorption with age,'' *J. Biomech.* **12**, 459–469 (1979).
10. Y. N. Yeni and T. L. Norman, ''Fracture toughness of human femoral neck: Effect of microstructure, composition, and age,'' *Bone (N.Y.)* **26**, 499–504 (2000).
11. P. Zioupos, J. D. Currey, and A. J. Hamer, ''The role of collagen in the declining mechanical properties of aging human cortical bone,'' *J. Biomed. Mater. Res.* **2**, 108–116 (1999).
12. X. Wang, X. Shen, X. Li, and C. M. Agrawal, ''Age-related changes in the collagen network and toughness of bone,'' *Bone (N.Y.)* **31**, 1–7 (2002).
13. C. U. Brown and T. L. Norman, ''Fracture toughness of human cortical bone from the proximal femur,'' *Adv. Bioeng.* **31**, 121–122 (1995).
14. W. Bonfield, J. C. Behiri, and C. Charalamides, ''Orientation and age-related dependence of the fracture toughness of cortical bone,'' in *Biomechanics: Current Interdisciplinary Research*, Martinum Nijhoff Publishers, Dordrecht, The Netherlands (1985).
15. X. D. Wang, N. S. Masilamani, J. D. Mabrey, M. E. Alder, and C. M. Agrawal, ''Changes in the fracture toughness of bone may not be reflected in its mineral density, porosity, and tensile properties,'' *Bone (N.Y.)* **23**, 67–72 (1998).
16. O. Akkus, F. Adar, and M. B. Schaffler, ''Age-related changes in physicochemical properties of mineral crystals are related to impaired mechanical function of cortical bone,'' *Bone (N.Y.)* **34**, 443–453 (2004).
17. J. D. Currey, K. Brear, and P. Zioupos, ''The effects of ageing and changes in mineral content in degrading the toughness of human femora,'' *J. Biomech.* **29**, 257–260 (1996).
18. R. K. Nalla, J. J. Kruzic, J. H. Kinney, and R. O. Ritchie, ''Effect of aging on the toughness of human cortical bone: Evaluation by R-curves,'' *Bone (N.Y.)* **35**, 1240–1246 (2004).
19. J.-Y. Rho, L. Kuhn-Spearing, and P. Zioupos, ''Mechanical properties and the hierarchical structure of bone,'' *Med. Eng. Phys.* **20**, 92–102 (1998).
20. S. Weiner and H. D. Wagner, ''The material bone: Structure-mechanical function relations,'' *Annu. Rev. Mater. Sci.* **28**, 271–298 (1998).
21. J. D. Currey, '' 'Osteons' in biomechanical literature,'' *J. Biomech.* **15**, 717 (1982).
22. R. K. Nalla, J. J. Kruzic, J. H. Kinney, and R. O. Ritchie, ''Mechanistic aspects of fracture and R-curve behavior in human cortical bone,'' *Biomaterials* **26**, 217–231 (2005).
23. R. Legros, N. Balmain, and G. Bonel, ''Age-related changes in mineral of rat and bovine cortical bone,'' *Calcif. Tissue Int.* **41**, 137–144 (1987).
24. C. Rey, V. Renugopalakrishnan, B. Collins, and M. J. Glimcher, ''Fourier transform infrared spectroscopic study of the carbonate ions in bone mineral during aging,'' *Calcif. Tissue Int.* **49**, 251–258 (1991).
25. A. L. Boskey, N. Pleshko, S. B. Doty, and R. Mendelsohn, ''Applications of Fourier transform infrared (FT-IR) microscopy to the study of mineralization in bone and cartilage,'' *Cells Mater.* **2**, 209–220 (1992).
26. N. P. Camacho, C. M. Rimnac, R. A. Meyer, Jr., S. Doty, and A. L. Boskey, ''Effect of abnormal mineralization on the mechanical behavior of x-linked hypophosphatemic mice femora,'' *Bone (N.Y.)* **17**, 271–278 (1995).
27. C. Rey, J. L. Miquel, L. Facchini, A. P. Legrand, and M. J. Glimcher, ''Hydroxyl groups in bone mineral,'' *Bone (N.Y.)* **16**, 583–586 (1995).
28. E. P. Paschalis, F. Betts, E. DiCarlo, R. Mendelsohn, and A. L. Boskey, ''Ftir microspectroscopic analysis of human iliac crest biopsies from untreated osteoporotic bone,'' *Calcif. Tissue Int.* **61**, 487–492 (1997).
29. J.-M. Very, R. Gibert, B. Guilhot, M. Debout, and C. Alexandre, ''Effect of aging on the amide group of bone matrix, measured by FTIR spectrophotometry, in adult subjects deceased as a result of violent death,'' *Calcif. Tissue Int.* **60**, 271–275 (1997).
30. N. P. Camacho, S. Rinnerthaler, E. P. Paschalis, R. Mendelsohn, A. L. Boskey, and P. Fratzl, ''Complementaty information on bone ultrastructure from scanning small angle x-ray scattering and Fourier-transform infrared microspectroscopy,'' *Bone (N.Y.)* **25**, 287–293 (1999).
31. E. P. Paschalis, K. Verdelis, S. B. Doty, A. L. Boskey, R. Mendelsohn, and M. Yamauchi, ''Spectroscopic characterization of collagen cross-links in bone,'' *J. Bone Miner. Res.* **16**, 1821–1828 (2001).
32. E. P. Paschalis, R. Recker, E. DiCarlo, S. B. Doty, E. Atti, and A. L. Boskey, ''Distribution of collagen cross-links in normal human trabecular bone,'' *J. Bone Miner. Res.* **18**, 1942–1946 (2003).
33. J. A. Timlin, A. Carden, M. D. Morris, J. F. Bonadio, C. E. Hoffler II, K. M. Kozloff, and S. A. Goldstein, ''Spatial distribution of phosphate species in mature and newly generated mammalian bone by hyperspectral Raman imaging,'' *J. Biomed. Opt.* **4**, 28–34 (1999).
34. O. Akkus, A. Polyakova-Akkus, F. Adar, and M. B. Schaffler, ''Aging of microstructural compartments in human compact bone,'' *J. Bone Miner. Res.* **18**, 1012–1019 (2003).
35. A. Carden, R. M. Rajachar, M. D. Morris, and D. H. Kohn, ''Ultrastructural changes accompanying the mechanical deformation of bone tissue: A Raman imaging study,'' *Calcif. Tissue Int.* **72**, 166–175 (2003).
36. R. Jyothi Lakshmi, M. Alexander, J. Kurien, K. K. Mahato, and V. B. Kartha, ''Osteoradionecrosis (orn) of the mandible: A laser Raman spectroscopic study,'' *Appl. Spectrosc.* **57**, 1100–1116 (2003).
37. G. Pezzotti and S. Sakakura, ''Study of the toughening mechanisms in bone and biomimetic hydroxyapatite materials using Raman microprobe spectroscopy,'' *J. Biomed. Mater. Res.* **65**, 229–236 (2003).
38. C.-K. Loong, C. Rey, L. T. Kuhn, C. Combes, Y. Wu, S.-H. Chen, and M. J. Glimcher, ''Evidence of hydroxyl-ion deficiency in bone apatites: An inelastic neutron-scattering study,'' *Bone (N.Y.)* **26**, 599–602 (2000).
39. M. G. Taylor, S. F. Parker, K. Simkiss, and P. C. H. Mitchell, ''Bone mineral: Evidence for hydroxyl groups by inelastic neutron scattering,'' *Phys. Chem. Chem. Phys.* **3**, 1514–1517 (2001).
40. A. Carden and M. D. Morris, ''Application of vibrational spectroscopy to the study of mineralized tissues (review),'' *J. Biomed. Opt.* **5**, 259–268 (2000).
41. R. Smith and I. Rehman, ''Fourier transform Raman spectroscopic studies of human bone,'' *J. Mater. Sci.: Mater. Med.* **5**, 775–778 (1995).
42. J. Bandekar, ''Amide modes and protein conformation,'' *Biochim. Biophys. Acta* **1120**, 123–143 (1992).
43. J. F. Knott, *Fundamentals of Fracture Mechanics*, Butterworth, London (1976).
44. B. R. Lawn, ''Physics of fracture,'' *J. Am. Ceram. Soc.* **66**, 83 (1983).
45. R. O. Ritchie, ''Mechanisms of fatigue crack propagation in metals, ceramics and composites: Role of crack-tip shielding,'' *Mater. Sci. Eng.* **103**, 15–28 (1988).
46. R. O. Ritchie, ''Mechanisms of fatigue-crack propagation in ductile and brittle solids,'' *Int. J. Fract.* **100**, 55–83 (1999).
47. A. G. Evans, ''Perspective on the development of high toughness ceramics,'' *J. Am. Ceram. Soc.* **73**, 187–206 (1990).
48. R. W. McCalden, J. A. McGeough, M. B. Barker, and C. M. Court-Brown, ''Age-related changes in the tensile properties of cortical bone. The relative importance of changes in porosity, mineralization, and microstructure,'' *J. Bone Jt. Surg., Am. Vol.* **75**, 1193–1205 (1993).
49. A. Bailey, R. G. Paul, and L. Knott, ''Mechanisms of maturation and ageing of collagen,'' *Mech. Ageing Dev.* **106**, 1–56 (1998).
50. A. J. Bailey, ''Molecular mechanisms of ageing in connective tissues,'' *Mech. Ageing Dev.* **122**, 735–755 (2001).
51. L. Knott and A. J. Bailey, ''Collagen cross-links in mineralizing tissues: A review of their chemistry, function, and clinical relevance,'' *Bone (N.Y.)* **22**, 181–187 (1998).
52. X. Li, C. M. Agrawal, and X. Wang, ''Age dependence of in situ thermostability of collagen in human bone,'' *Calcif. Tissue Int.* **72**, 513–518 (2003).
53. A. J. Bailey, T. J. Sims, E. N. Ebbesen, J. P. Mansell, J. S. Thomsen, and L. Mosekilde, ''Age-related changes in the biochemical properties of human cancellous bone collagen: Relationship to bone strength,'' *Calcif. Tissue Int.* **65**, 203–210 (1999).
54. X. Wang, X. Li, X. Shen, and C. M. Agrawal, ''Age-related changes of noncalcified collagen in human cortical bone,'' *Ann. Biomed. Eng.* **31**, 1365–1371 (2003).
55. D. R. Eyre, M. A. Paz, and P. M. Gallop, ''Cross-linking in collagen and elastin,'' *Annu. Rev. Biochem.* **53**, 717–748 (1984).